Supplementary Information

Formation of MoO_3 and WO_3 Nanoscrolls from MoS_2 and WS_2 by Atmospheric Air Plasma

Ximo S. Chu,[a] Duo O. Li,[a] Alexander A. Green,[b] and Qing Hua Wang*[a]

[a] Materials Science and Engineering, School for Engineering of Matter, Transport and Energy, Arizona State University, Tempe, AZ 85287, United States

[b] Biodesign Center for Molecular Design and Biomimetics, The Biodesign Institute, and the School of Molecular Sciences, Arizona State University, Tempe, AZ, USA, 85287

* Corresponding author:

qhwang@asu.edu

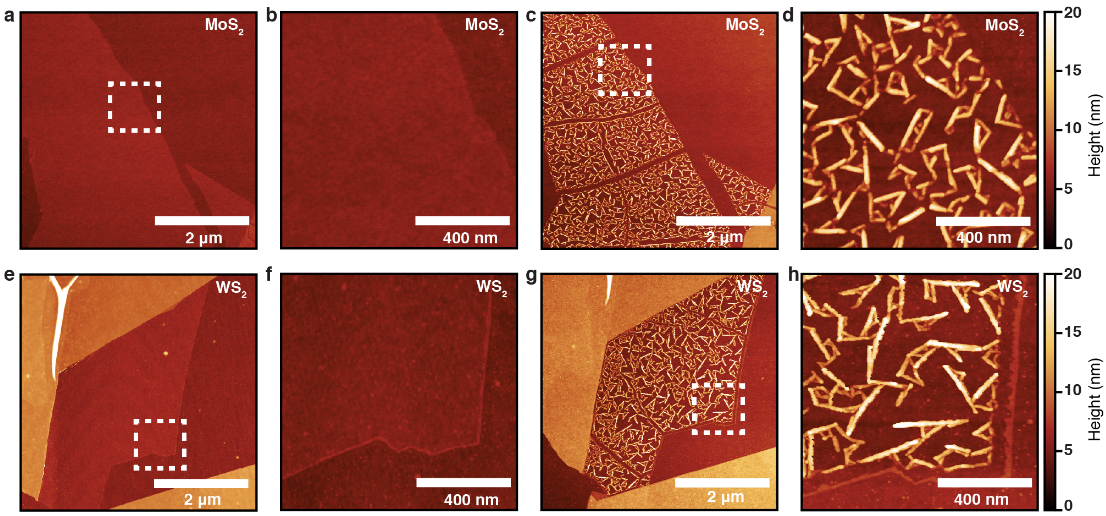

Figure S1: Nanoscroll formation after air plasma treatment of MoS_2 and WS_2. Atomic force microscopy (AFM) images of MoS_2 and WS_2 before and after air plasma treatment. **(a)** AFM image of monolayer MoS_2 as exfoliated, and **(b)** magnified in the area in the dashed box in (a). **(c)** AFM image in the same area as (a) after 2 s air plasma treatment, and **(d)** magnified in the area in the dashed box in (c). **(e)** Monolayer WS_2 as exfoliated and **(f)** magnified in the area in the dashed line box in (e). **(g)** The same area as (e) after 2 s air plasma treatment and **(h)** magnified in the area in the dashed box in (g).

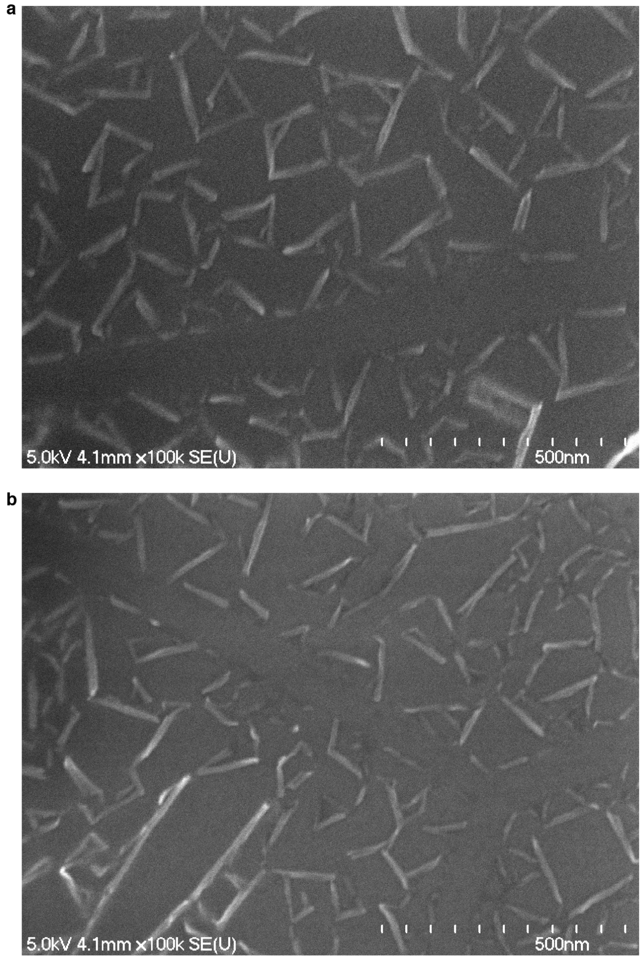

Figure S2: Field emission scanning electron microscopy (FESEM) images of MoO_3 nanoscrolls. The FESEM was conducted using a Hitachi S4700 system. Panels (a) and (b) show nanoscrolls in different regions of a sample. The nanoscroll features are similar to those seen in AFM images.

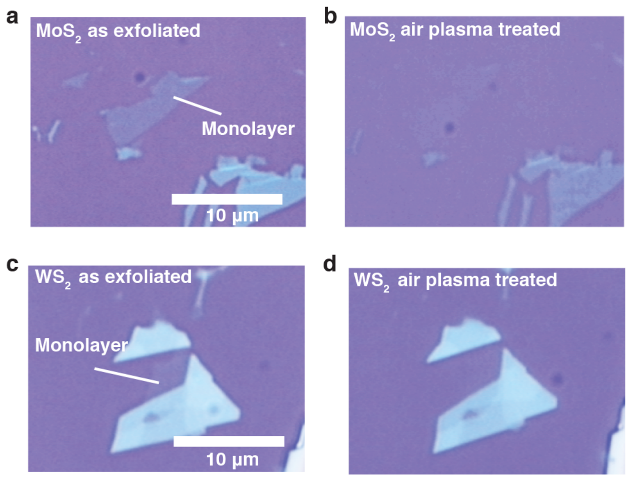

Figure S3: MoS_2 and WS_2 optical microscope images before and after air plasma treatment. (a) Optical microscope image of as exfoliated MoS_2 and **(b)** the same region after air plasma treatment. **(c)** Optical microscope image of as exfoliated WS_2 and **(d)** the same region after air plasma treatment. After air plasma treatment of both materials, the monolayers are nearly invisible.

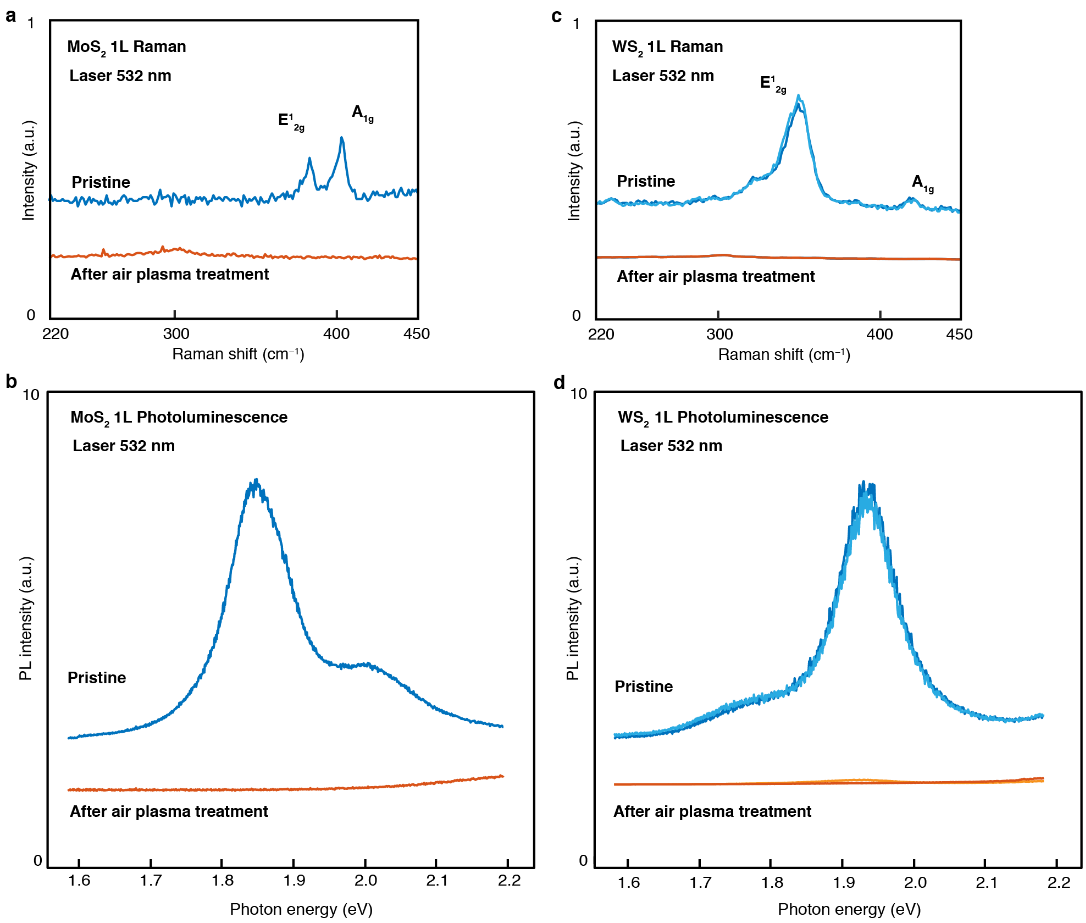

Figure S4: Raman and PL spectra for monolayer MoS_2 and WS_2. (a) Raman spectra for pristine mechanically exfoliated monolayer MoS_2 and in the same region after air plasma treatment. The distance between the characteristic E^1_{2g} and A_{1g} peaks in the pristine MoS_2 sample is 19 cm^{-1}. The peaks are no longer present after plasma treatment. **(b)** Photoluminescence (PL) spectra for pristine monolayer MoS_2 and the same region after air plasma treatment. After air plasma, the PL peaks are gone. **(c)** Raman spectra for pristine mechanically exfoliated monolayer WS_2 and in the same region after air plasma treatment. The characteristic E^1_{2g} and A_{1g} peaks are marked. **(d)** PL spectra for monolayer WS_2 and the same region after air plasma treatment.

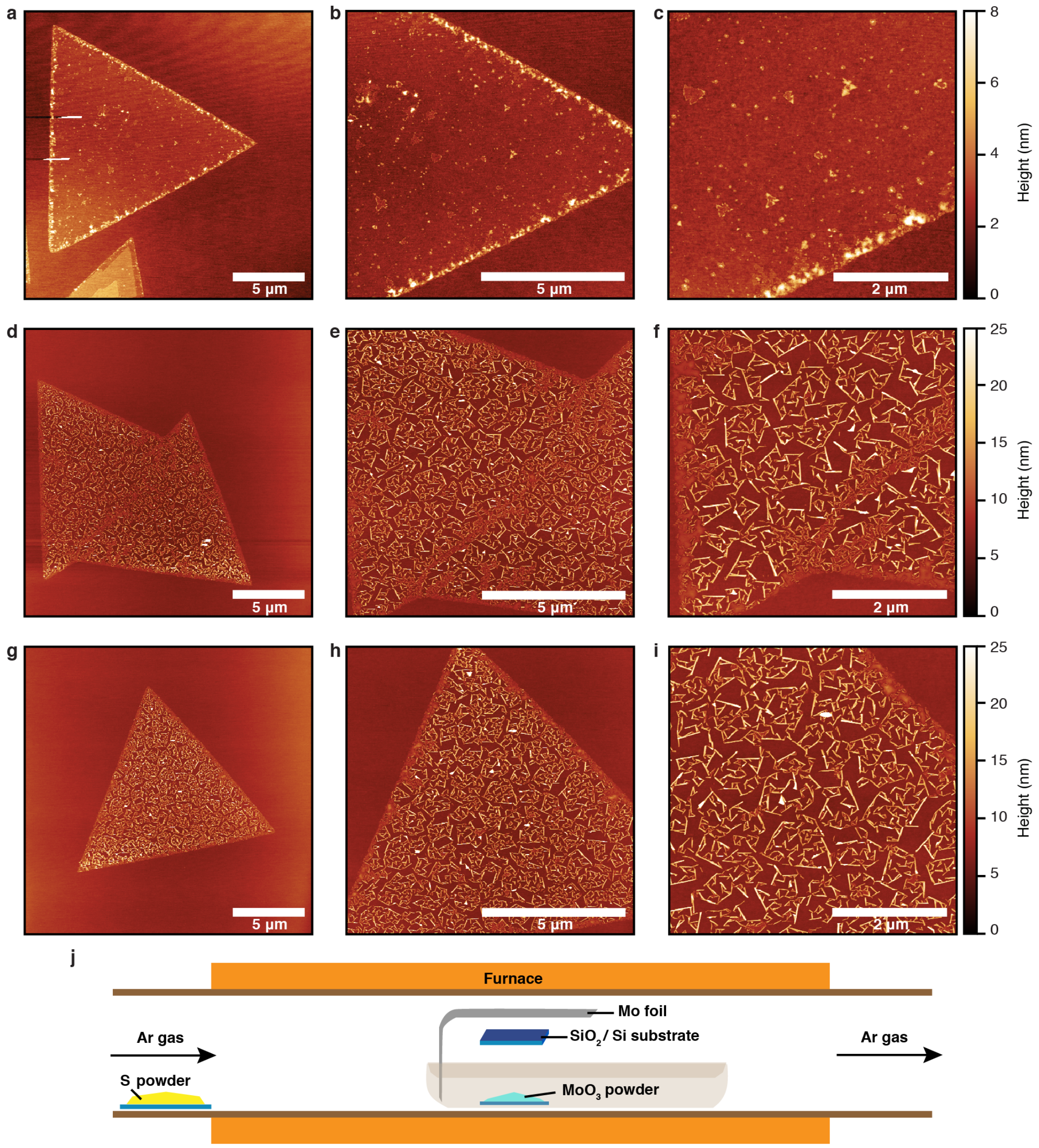

Figure S5: Formation of nanoscrolls in single crystal CVD-grown MoS_2. (a)-(c) AFM images of single crystal MoS_2 after CVD growth. Images show increasing magnification of the same sample. **(d)-(i)** AFM images of MoS_2 after 2 s air plasma treatment showing formation of nanoscrolls. Images (d)-(f) show the same sample with increasing magnification, and images (g)-(i) show the same sample with increasing magnification. **(j)** Schematic illustration of experimental setup for CVD growth of single crystal MoS_2.

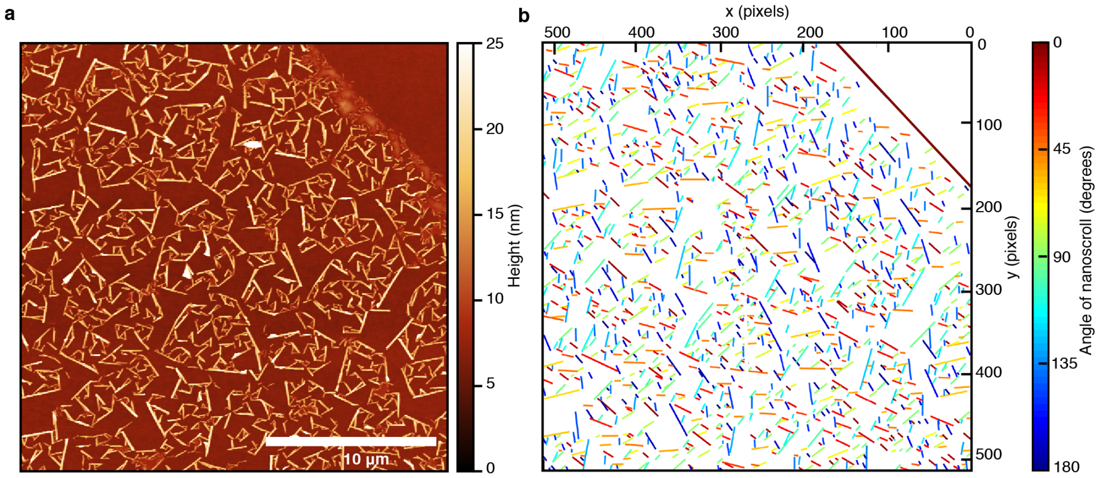

Figure S6: Image analysis for nanoscroll orientations. (a) Single crystal MoS_2 after 2 s air plasma treatment. **(b)** Each nanoscroll has been marked as a line segment, along with the edge of the original MoS_2 crystal. The color of each line corresponds to its angle with respect to the MoS_2 edge.

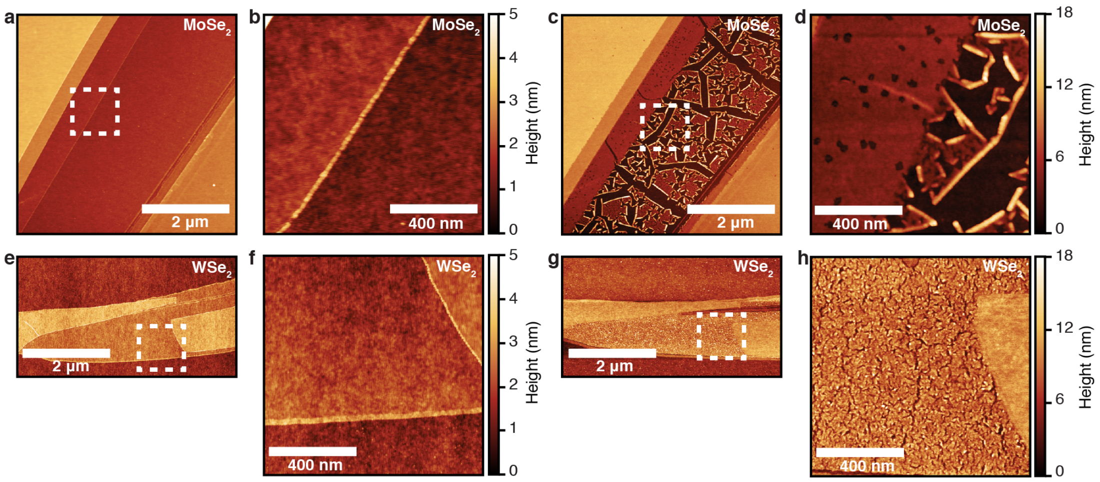

Figure S7: Air plasma treatment of $MoSe_2$ and WSe_2. (a)-(b)AFM images of $MoSe_2$ as exfoliated (**(b)** shows the area marked by the dashed square in (a)), and **(c)-(d)** after 2 s air plasma treatment. Some nanoscrolls have formed in the monolayer region (**(d)** shows the area marked by the dashed square in (c)). **(e)-(f)** AFM images of WSe_2 as exfoliated (**(f)** shows the area marked by the dashed square in (e)), and **(g)-(h)** after 2 s air plasma treatment (**(h)** shows the area marked by the dashed square in (g)). No nanoscrolls have formed, but there are some cracks.

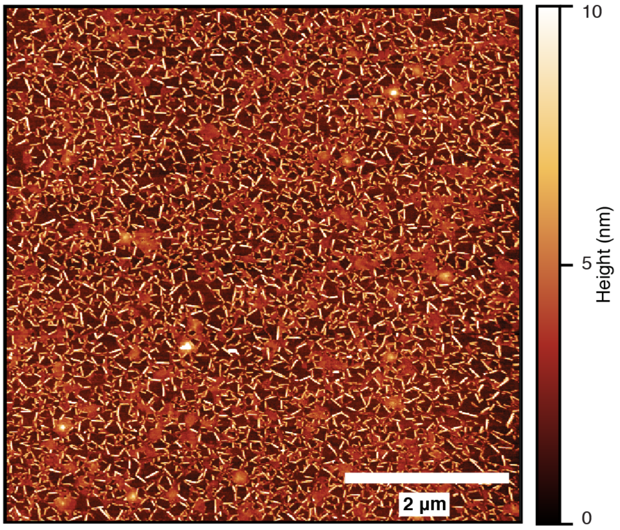

Figure S8: Nanoscroll formation in large-area CVD-grown MoS_2 after air plasma treatment. A large-area continuous film of monolayer MoS_2 was grown by chemical vapor deposition (CVD). After the same air plasma treatment that was applied to other samples, nanoscrolls are also formed, as shown in the AFM image here.

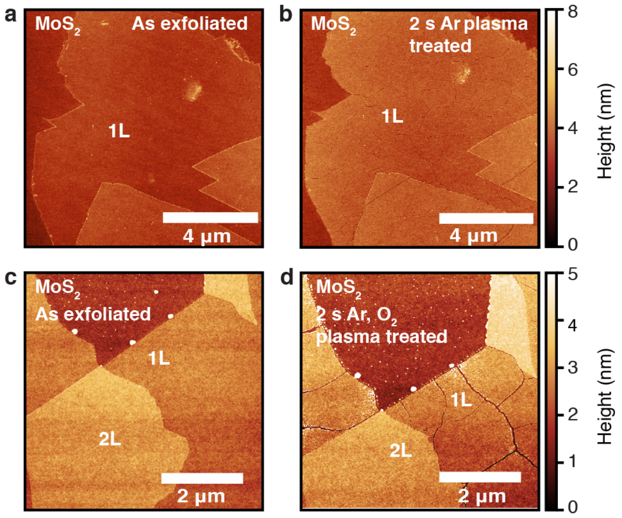

Figure S9: MoS_2 after Ar plasma and Ar/O_2 gas mixture plasma. (a) AFM image of MoS_2 as exfoliated and **(b)** after 2 s Ar plasma treatment. **(c)** AFM image of MoS_2 as exfoliated and **(d)** after Ar/O_2 gas mixture plasma treatment. In both cases, nanoscrolls do not form.

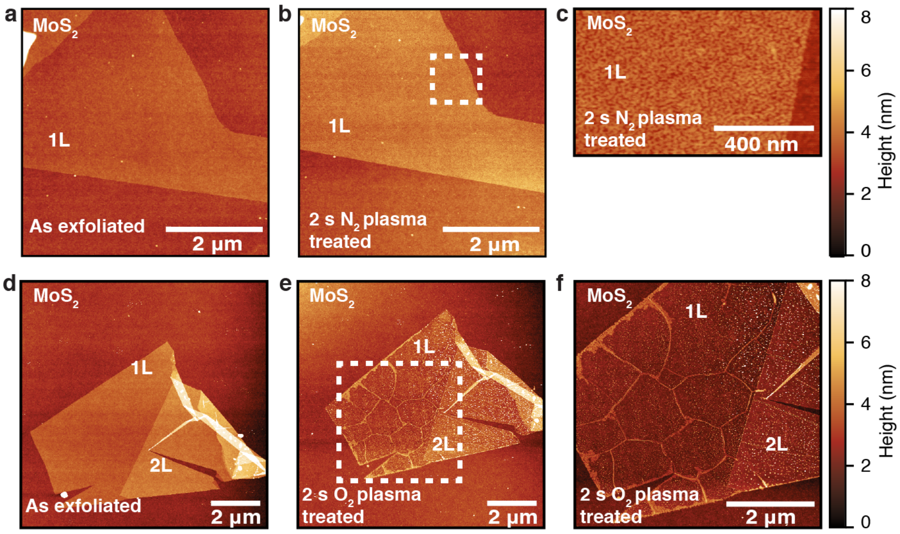

Figure S10: MoS_2 after N_2 plasma treatment and after O_2 plasma treatment. (a), (d) AFM images of different MoS_2 samples as exfoliated, **(b)-(c)** after 2 s N_2 plasma treatment, and **(e)-(f)** after 2 s O_2 plasma treatment. In both cases, nanoscrolls do not form, but there is an increase in roughness with N_2 plasma, and cracks and increasing height with O_2 plasma.

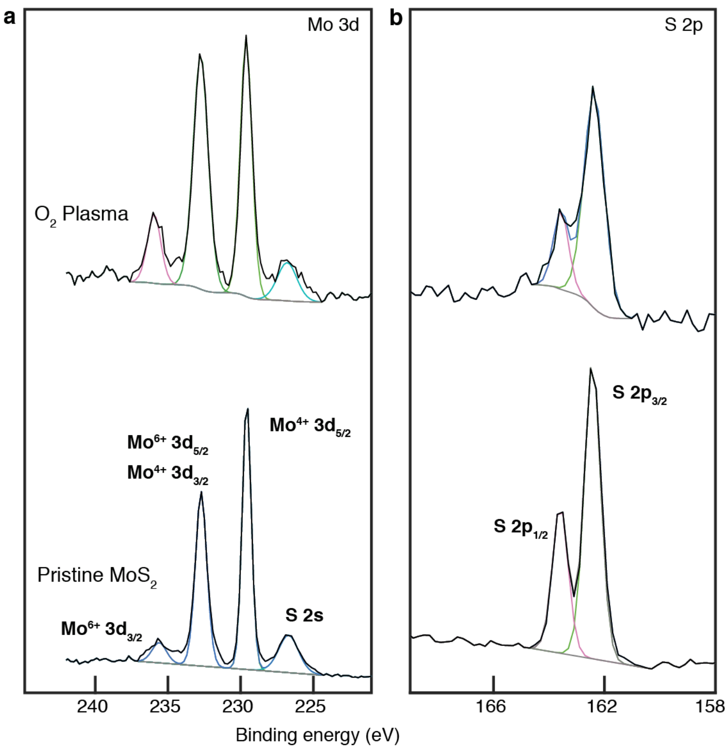

Figure S11: X-ray photoelectron spectroscopy (XPS) of pristine MoS_2 and treated by O_2 plasma. Lower spectrum: pristine MoS_2. Upper spectrum: after O_2 plasma treatment. **(a)** Peaks in Mo 3d region. **(b)** Peaks in S 2p region.

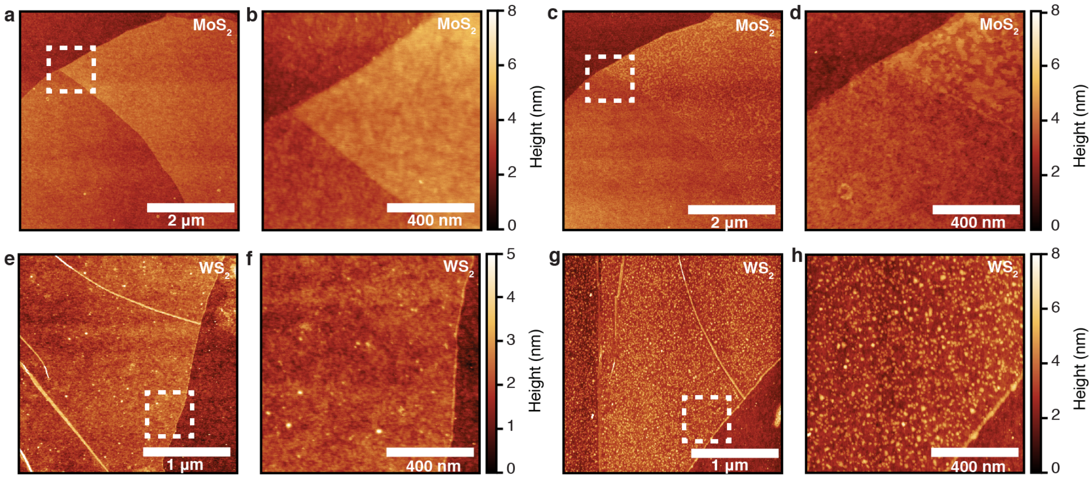

Figure S12: MoS_2, and WS_2 samples after plasma treatment with an N_2/O_2 gas mixture. (a)-(b) AFM images of MoS_2 as exfoliated (**(b)** shows the area marked by dashed square in (a)), and **(c)-(d)** after 2 s N_2/O_2 gas mixture plasma treatment (**(d)** shows the area marked by dashed square in (c)). **(e)-(f)** AFM images of WS_2 as exfoliated (**(f)** shows the area marked by dashed square in (e)), and **(g)-(h)** after 2 s N_2/O_2 gas mixture plasma treatment. No nanoscrolls have formed in either material.

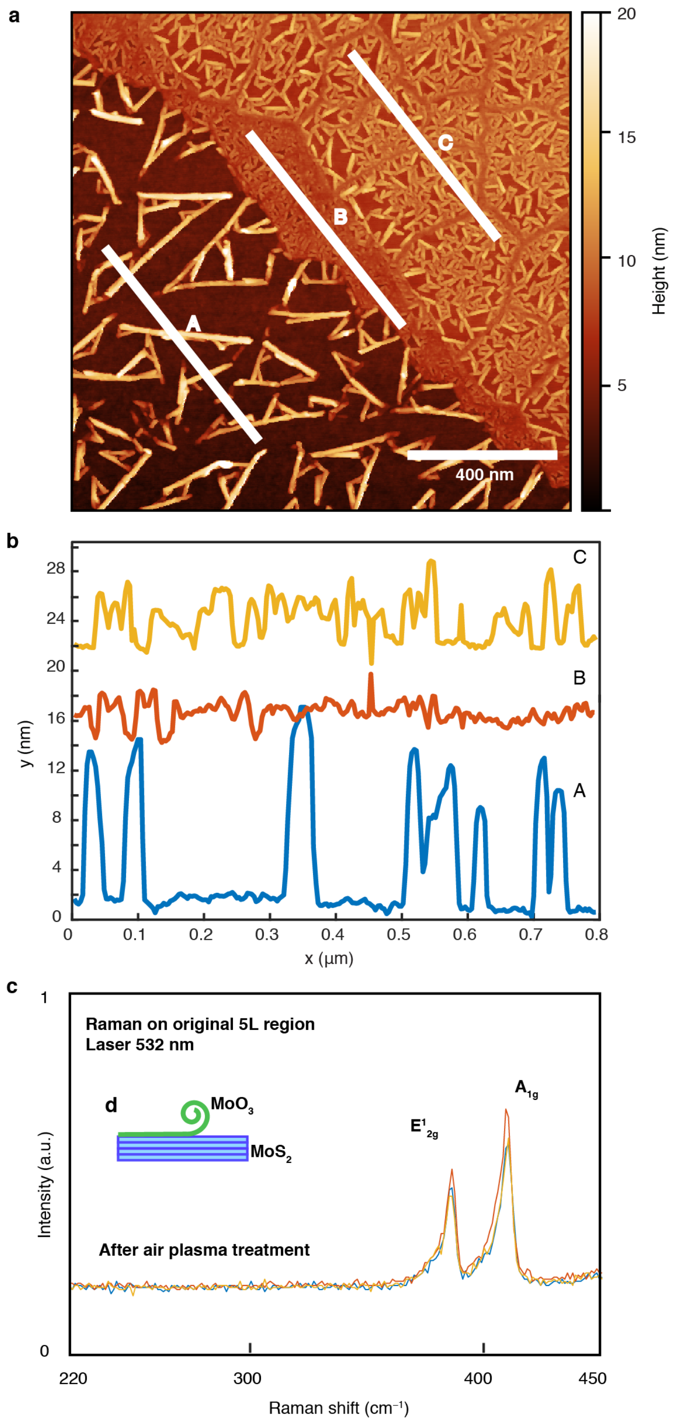

Figure S13: Formation of nanoscrolls on multilayered MoS_2. (a) AFM image showing formation of nanoscrolls after air plasma treatment of MoS_2 flake with different initial layer numbers. The lines A, B, and C correspond to regions where the initial thicknesses were 1L, 3L and 5L, respectively. **(b)** Height profiles along lines A, B, and C. Profiles are vertically offset for clarity. The thickness changes due to air plasma treatment suggest that only the top layer of the multilayer MoS_2 rolls up. **(c)** Raman spectra for the multilayer (5L) region after air plasma treatment. The characteristic peaks for MoS_2 are still clearly visible because only the top layer is oxidized. **(d)** Schematic illustration showing air plasma treatment only causes the top layer to oxidize and roll into MoO_3 nanoscroll, while the remaining material remains as MoS_2.

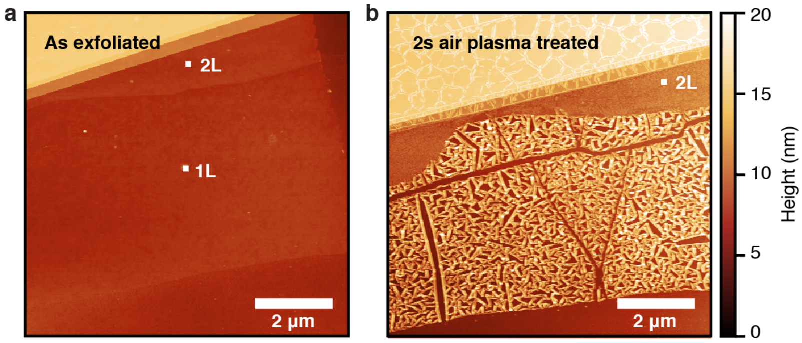

Figure S14: Nanoscroll formation of monolayer, bilayer, and multilayered MoS_2. (a) AFM images of MoS_2 as exfoliated with monolayer (1L) and bilayer (2L) regions marked, and **(b)** after 2 s air plasma treatment. The 2L labels indicate the same position on a bilayer region in panels (a) and (b). In the monolayer (1L) region, nanoscrolls have formed. There are no cracks or nanoscrolls in the bilayer (2L) region. There are cracks and nanoscrolls in the multilayer (>3L) region.

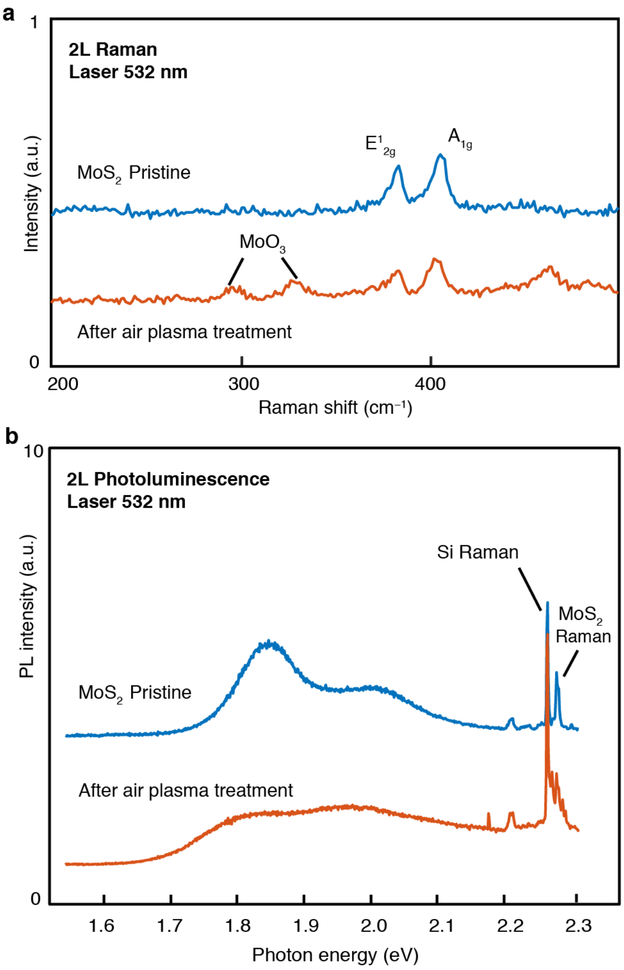

Figure S15: Raman and PL spectra for bilayer MoS_2. (a) Raman spectra for pristine bilayer MoS_2 and in the same region after air plasma treatment. The characteristic E^1_{2g} and A_{1g} peaks are still visible after plasma treatment, and new peaks from MoO_3 appear. **(b)** PL spectra for pristine bilayer MoS_2 and the same region after air plasma treatment. After air plasma, the PL peaks are significantly lower in intensity.